Quantum mechanical effects in *n*-alkane droplets

Rasoul Nasiri[1], Vladimir M Gun'ko[2], Sergei S Sazhin[1]

[1]Sir Harry Ricardo Laboratories, School of Computing, Engineering and Mathematics,
University of Brighton, Brighton BN2 4GJ, UK
[2]Chuiko Institute of Surface Chemistry, 17 General Naumov Street, Kiev 03164, Ukraine

Abstract

According to quantum chemical (QC) calculations of a series of *n*-alkanes (C_nH_{2n+2} at n = 1-8) the gap Δ_{HL} between the highest occupied molecular orbital (HOMO) and the lowest unoccupied molecular orbital (LUMO) decreases with increasing methylene group (-CH_2-) number in the *n*-alkane chain. While the LUMO level appears to be relatively unchanged, in good agreement with experimental results, the HOMO level is unstabilized and Δ_{HL} decreases from approximately 11 eV (methane) to 6.5 eV (*n*-octane). Comparative *ab initio* calculations show not only the quantum confinement effects (QCE) in *n*-alkanes in the gas phase due to the reduction of the Δ_{HL} value, but also enabled selection of cost-effective methodologies for modelling long-chain *n*-alkanes ($n > 8$). The used methodologies include 'Local Spin Density Approximation', combining special exchange functional with suitable correlation functional. Electronic structures and energetics of *n*-pentane (C_5H_{12}) in the evaporation/condensation processes are studied to understand the molecular mechanism for these processes. Two main step processes, liquid (L) $\overset{1}{\rightleftharpoons}$ liquid-gas (L-G) interface $\overset{2}{\rightleftharpoons}$ gas (G), are analysed. While phase transformations between L and L-G is estimated as activation processes, it is found that there is no energy barrier in the transitions between L-G and G.

1- Introduction

N-alkanes (C_nH_{2n+2} at $n > 4$) are the main compounds in Diesel and petrol fuels. Due to a wide range of applicability of *n*-alkanes in science (1) and engineering (2), many groups have tried to develop or refine various molecular models for studying alkanes in the gas and liquid states using quantum chemistry (QC) (3, 4), all atom force field (AAFF) (5-7), united-atom force field (UAFF) (8, 9) and coarse-graining force field (CGFF) (10) methods. The resolutions of these approaches change from electronic structures (QC) to beads (a set of united atoms) in CGFF. Both QC and classical models are powerful methods for investigations of alkane chemistry and physics at molecular level. They can deal with various timescales, system sizes and related quantum effects. While advanced QC methods are based on *many-body* interactions of electrons and nuclei, classical force fields can describe interaction of particles (atoms, united atoms and beads) via *pair-wise* electrostatic, hydrogen bonding, and van der Waals potentials. Note that pure QC methods can give ground state properties (T = 0 K), and the temperature dependent properties such as enthalpy of vaporization can be estimated using the quantum thermo-chemical (QTC) calculations. An alternative approach can be based on Molecular Dynamics/Monte Carlo (MD/MC) (with (QC) or without (FF) consideration of electrons and nuclei) simulation algorithms in which thermal effects are taken into account.
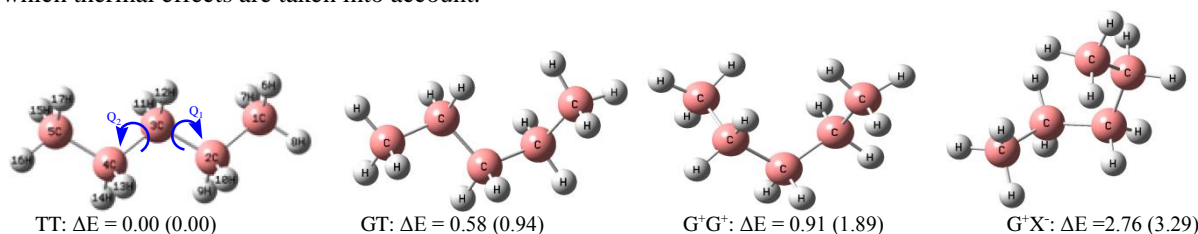

TT: ΔE = 0.00 (0.00)   GT: ΔE = 0.58 (0.94)   G⁺G⁺: ΔE = 0.91 (1.89)   G⁺X⁻: ΔE =2.76 (3.29)

Figure 1 Structures and relative energies (kcal/mol) of four isomers of *n*-pentane obtained using QC and FF methods. T refers to the trans conformer with dihedral angles $\varphi_{1,2}$ = ±180°, G refers to gauche torsion with $\varphi_{1,2}$ = ±60°, X refers to $\varphi_{1,2}$ = ±90°. φ_1 refers to the angle between the planes 1C-2C-3C and 2C-3C-4C; φ_2 refers to the angle between the planes 2C-3C-4C and 3C-4C-5C (see the left-hand side scheme).

Traditionally evaporation and condensation of *n*-alkane droplets have been investigated using MD/UAFF simulations (11, 12). In these processes it is essential to take into account the influence of conformational changes caused by temperature and dynamical interactions. Since the energy difference between most conformers of *n*-alkanes is about 1-3 kcal/mol, capturing these conformers by UAFFs or even AAFFs would be challenging. Energies of four isomers of C_5H_{12} (Figure 1) calculated using Coupled-Cluster with Single and Double Excitations /correlation consistent-polarized Valence Triple Zeta (CCSD (T)/cc-pVTZ) (13) and AAFF

(Optimized Potentials for Liquid Simulations - All Atom (OPLS-AA)) (5) (shown in the brackets) are essentially different in QC and force field methods.

For OPLS-AA-FF energies the relative errors are in the range from 20 to 100%. While QC calculations show the values of mole fractions of 0.282, 0.673, 0.034 and 0.011 for conformers of TT, GT, G^+G^+ and G^+X^+ respectively (14), the calculations based on the molecular mechanics (MM) method for the same conformers at 300 K lead to rather different values: 0.491, 0.436, 0.064 and 0.009 (15). Using OPLS-AA-FF, Jorgensen's group (5) identified $C_{22}H_{46}$ as the smallest and most stable *n*-alkane with hairpin (folded) geometry, while Suhm et al. (16) showed, using QC methods and Raman spectroscopy techniques, that $C_{17}H_{36}$ is the starting point for *n*-alkanes with the folded structure. There is balance between intra- and intermolecular interactions in these molecules (16). These conflicting results have stimulated our interest in finding a suitable method to study the effects of conformational changes or isomerizations of alkanes. We believe that analysis of these effects is important for clarifying the molecular mechanism of the evaporation/condensation processes.

An MC statistical mechanics simulation has shown that *n*-alkanes (from C_4H_{10} to $C_{12}H_{26}$) stay in anti-conformations with two gauche bonds per molecule in the gas phase and pure liquid (5). In this study OPLS-AA was applied to a series of these alkanes. Obtained results are in excellent agreement with experimental data. Enthalpy of evaporation of *n*-dodecane obtained using MC simulation and experimental methods were reported to be 16.28 and 14.65 kcal/mol, respectively. Siu et al. (6) developed a revised version of OPLS-AA for long chain hydrocarbon molecules using MD simulation techniques, called L-OPLS-AA, in which intra-molecular parameters of the force field are refitted using high level *ab initio* calculations. The results were in better agreement with experimental data in comparison with the results reported in (5): 22.27 and 14.59 kcal/mol for enthalpy of vaporization of *n*-dodecane by OPLS-AA and L-OPLS-AA, respectively.

None of these force fields are suitable for modelling of *n*-alkanes at high temperatures (internal combustion engine conditions) since those have been developed for simulation of biomolecules. Siepmann's group developed a series of novel FFs named TraPPE (Transferable Potentials for Phase Equilibria) for modelling the vapour-liquid equilibrium of hydrocarbons (alkanes, cycloalkanes, alkylbenzenes, polycyclics and their mixtures) (9, 17-25). These FFs were parameterized to the experimental values of heat of evaporation and density in both gas and liquid phases. Although the TraPPE FFs could provide significant progress in modelling of *n*-alkanes over a wide range of thermodynamic conditions (temperature and pressure) using various resolutions (AA, UA and CG) (19, 20, 24), they could not take into account the effects of the detailed electronic structures of *n*-alkanes during such processes as evaporation/condensation. Knowledge of electronic structures allows one to find an answer to the questions: why does the HOMO-LUMO gap in alkanes decrease when their backbone becomes longer? What are the changes in energies and structures of alkanes during evaporation/condensation from the liquid (L) into the gas (G) state and what are the features of the processes at the liquid-gas (L-G) interface? Part of the second question might be answered using classical FFs such as TraPPE but without consideration of quantum effects caused by changes in the electronic structure. Therefore, in this study, we focus on the electronic structures of *n*-alkanes.

The focus of the paper is on comparative quantum chemical (QC) calculations for *n*-alkanes. In the first part of the paper, a series of short *n*-alkanes (*n* = 1-8) in the gas phase is considered in order to respond to the question Why does the HOMO-LUMO gap decrease as the number of carbons (*n*) in the chain of alkanes increases? In the second part, we will try to extend our calculations to *n*-pentane molecule in the liquid phase to find out whether transformation of the molecule from the liquid phase to the gas phase, or the inverse of this, is a single step process or whether it includes several steps for evaporation/condensation from/to a droplet. These results will provide new insight into the evaporation/condensation of droplets taking into account changes in the *n*-alkane electronic structures during evaporation/condensation. The results will be shown to be in good agreement with experimental observations (25-27).

2- Method of analysis and computational scheme

All calculations were performed using Gaussian 09 (28), WinGAMESS (version 11 Aug 2011 (R1)) (29) and GaussView program for visualization (30). Several QC approaches, such as the second-order Møller-Plesset (MP2) perturbation theory, Density Functional Theory (DFT), Semiempirical Quantum Chemical (SQC) and Hartree Fock (HF) methods, were applied to the analysis of alkanes in the gas phase (Figure 2). QC calculations in the liquid phase were performed using an improved SQC potential called the Pairwise Distance Directed Gaussian (PDDG) function (31). In order to find out the relationship between the HOMO-LUMO gap and electronic structures of several conformers in *n*-alkanes, a setup was prepared to evaluate the effect of conformational changes (rotation of the atoms or united atoms around the single C-C bonds) on the molecular orbital bands (MOBs). Two torsion angles φ_1 and φ_2 (Figure 1) in the backbone of *n*-pentane molecule were scanned in 10 degree increments using the PDDG/PM3 potential. This gave 36×36 stationary points for *n*-pentane molecule over the potential energy hypersurface. While these dihedral angles were constrained for each point, other remaining internal parameters were optimized. This allowed us to identify the locations of all minima, transition states and even second-order saddle points over the PES (Figure 3).

Using the same potential, a relaxed SCAN on the PES was also used for the analysis of attachment/detachment of *n*-pentane molecule from/to the slab ($18C_5H_{12}$) (see Figure 4a) to identity of the reactants and products corresponding to each TS structure during the evaporation. The profile energy is presented in Figure 4b. Note the SQC is not considered to be reliable for quantitative determination of the activation barriers, providing only useful qualitative information on the PES (position of stationary points on the PES). Our conformational analyses are limited to SQCs.

For validation of the PDDG/PM3 function and selection of the best potential, inter- and intra-molecular interactions were compared with CCSD (T)/cc-pVTZ results. The results of comparison of intermolecular interactions C_3-C_{12} are shown in Table 2. The relative errors in the electronic energies of *n*-pentane molecule as a function of two torsion angles using PDDG/PM3 are shown in Figure 4. We followed this strategy to find out which would be a cost effective QC potential/method for studying the evaporation/condensation dynamics at the level of electronic structures.

3-   Results

This section shows energies and structures of alkanes in both gas and liquid phases. First, the structures of a series of the *n*-alkanes (*n*=1-8) were fully optimized in the gas phase for evaluation of the HOMO-LUMO gap using various QC methods and basis sets. It is shown in Figure 2 that the HOMO-LUMO gap decreases by about 5 eV when the length of the *n*-alkane chain increases. To find out the reason for this we have investigated the relationship between conformational changes of *n*-alkanes and their MOBs. We started with QC calculations for selected *n*-alkanes in the gas phase.
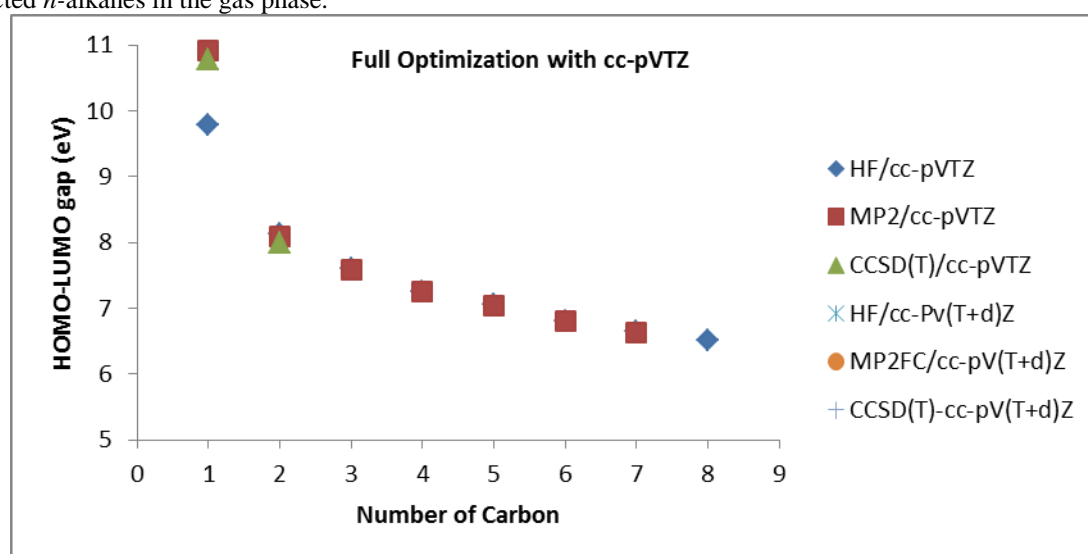

Figure 2. The values of the OMO-LUMO gap versus the number of carbon atoms in *n*-alkanes (C1-C8).

3-1 QC calculations in the gas phase

Using the results discussed above, a setup was prepared for studying inter- and intra-molecular interactions in alkanes. We compared them with high level *ab initio* potentials (MP2 and CCSD (T)) to find the best potential for studying of evaporation of *n*-alkanes. Firstly we calculated the interaction energies between two identical molecules (C_3-C_{12}). The results are shown in Table 1. In contrast to the semiempirical potentials of PM6 and AM1, the PDDG/PM3 potential has a good agreement with MP2 results. The HF methods and some conventional DFT were also unable to produce accurate results. Therefore, PDDG/PM3 could be considered reliable for estimating the inter-molecular interactions between *n*-alkane molecules only for the trans-conformer which is the most stable conformer among others (see conformer TT in Figure 1 and compare it with other cases).

In our analysis, we relied on the most stable conformation of *n*-alkanes (all-trans) for studying inter-molecular interactions and considered the effects of other conformers in the following part of the study in which intra-molecular interactions are discussed in detail. Recent QC studies of *n*-butane, *n*-pentane, and *n*-hexane molecules showed that the contribution of trans-conformers rapidly decreases with increasing temperature and the contribution of others increases with increasing temperatures from 100 to 500 K (33-36). The same authors established experimentally and theoretically that conformational changes strongly affect MOBs of *n*-alkanes. This encouraged us to search for all conformers of one of the *n*-alkanes using the PDDG/PM3 semiempirical potential in QC calculations.

The range of variations of electronic energies was determined for all stationary points of *n*-pentane molecule, as a representative of *n*-alkanes, using the PDDG/PM3 potential. We found four minima, six transition states that

connect minima and four second-order saddle points that connect all TSs. This could be a hint for clarification of the conformational energy-dependent HOMO-LUMO gap. As can be seen from Figure 3a, the value of the relative electronic energy increased up to 17 kcal/mol which corresponds to the energy of the second-order saddle point conformer. This value would be larger for longer alkanes since the number of conformers dramatically increases with increasing length of the backbone of *n*-alkanes (the number of nonequivalent minima conformers for C_5H_{12}, C_6H_{14}, C_7H_{16} and C_8H_{18} are 4, 12, 30 and 95 respectively). The relative values of energy for one of the stable conformers increase from 2.76 kcal/mol for G^+X^- isomer of *n*-pentane to 4.92 kcal/mol for $X^-G^+X^-$ isomer of *n*-hexane and to 8.08 kcal/mol for $L^+G^+X^-G^+X^-$ isomer of *n*-octane (37). Moreover, since the LUMO level was shown to be relatively unchanged, in good agreement with experimental results (25-27), it can be concluded that conformer isomerization (*conformerization*) can lead to a decreasing HOMO-LUMO gap.

Table 1. Comparison of inter-molecular interaction energies (kcal/mol) in *n*-alkanes

Molecule	PDDG/PM3	MP2/cc-pVTZ*	PM6	AM1	HF/ 6-31G**	DFT_B97D/ 6-31G**	OPBE/ 6-31G**	OPBESOL/ 6-31G*)
C12	-10.2	-10.5	-2.7	0.0	-0.2	-8.3	-0.6	-1.9
C11	-9.3	-9.6						
C10	-9.7	−8.75						
C9	-7.3	−7.75						
C8	-5.9	−6.68						
C7	-5.5	−5.96						
C6	-4.5	−4.91						
C5	-3.6	−3.92						
C4	-3.1	−2.97						
C3	-2.0	−2.08						

*Data collected from [32]. MP2 results were in good agreement with CCSD (T)/cc-pVTZ (see [32]).

For validation of the PDDG/PM3 potential, we compared intra-molecular interactions of *n*-pentane with high level *ab initio* calculations to find out whether the calculated values of energy can be reliable. The results showed that PDDG/PM3 fails in reproducing CCSD (T)/cc-pVTZ results since relative errors reached ±3 kcal/mol (see Figure 3b). This issue is related to all SQC methods; these cannot locate TSs correctly on the potential energy hypersurface. The main reasons for this are related to the unusual nature of the TS structures and also their properties which are not available from experiments. Moreover, according to (38), none of the semiempirical potentials can model activation barriers accurately since estimation of the barriers requires a high degree of accuracy in basis sets (SQCs are in the lowest levels of the basis sets). An error of ~1.5 kcal/mol in the estimation of interaction energies led us to more than one order of magnitude overestimation in the rate of evaporation (39). The intra-molecular interactions have significant effects on the evaluation of activation energies during the evaporation process.
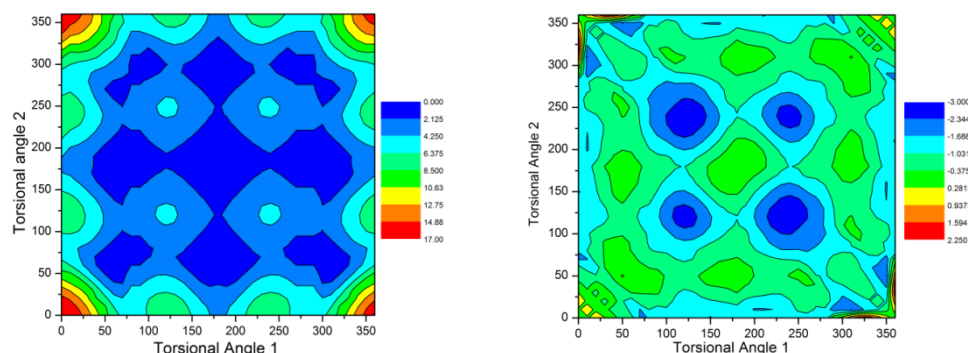

Figure 3 (a-left hand side) Contours of relative energies (kcal/mol) of *n*-pentane molecule obtained using the PDDG function; (b-right hand side) relative errors (kcal/mol) of the PDDG/PM3 potential in the PES of *n*-pentane molecule.

Martine's group recently developed a double-hybrid DFT in which exchange and correlation effects are taken into account along with spin component contributions and dispersion effects (40). This potential could reproduce inter- and intra-molecular interaction energy values in good agreement with high level *ab initio* methods; the reported errors were less than 0.2 kcal/mol which is better than the chemical accuracy (13). The essential point for our modelling is applicability of a suitable potential that can model conformational changes properly. We

find that DSD-PBEP86-D$_2$ has these specifications for our molecules (see (41-44) for details). Therefore, DSD-PBEP86-D$_2$ is suggested as a cost-effective potential for studying alkanes in both gas and liquid phases at a reasonable computational cost.

3-2 Liquid phase

In this part of the paper, we describe structurally and energetically the removal of *n*-pentane molecule from a slab of 18 *n*-pentane molecules (Figure 4). Before starting QC calculations, we optimized the structure of the slab using OPLS-AA force field. This gave us an initial conformer in which molecules were in a zigzag shape (all-trans form) and the distances between their centres of mass were about 0.4 nm. This structure is labelled **Re** in Figure 4.
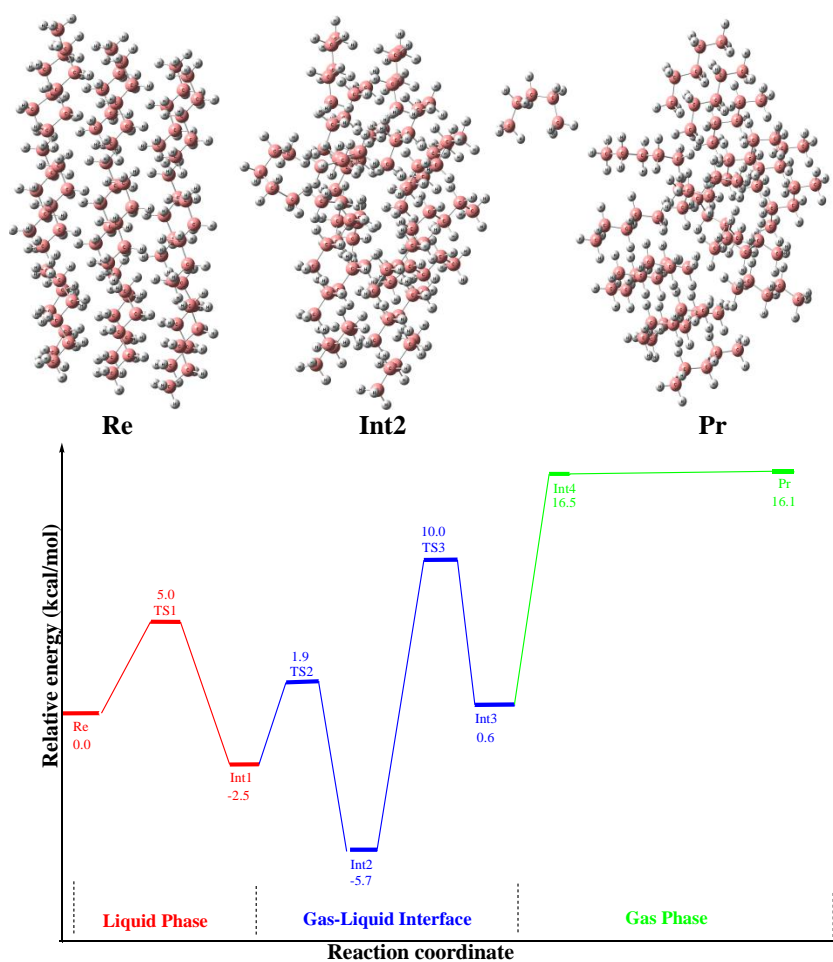

Figure 4 (a) Structures of the initial (**Re**), the most stable intermediate (**Int2**) and final products (**Pr**) of *n*-pentane slab in L, L-G and G, respectively. **(b)** Energy profile of removal of *n*-pentane molecule from the slab (all values of energies were calculated based on the PDDG/PM3 potential, kcal/mol).

A specific technique was applied for obtaining energies and structures of alkanes during the evaporation in the liquid phase (L), liquid-gas (L-G) interface and gas phase (G). A reaction coordinate was defined as a distance along the normal to the plane formed by the centres-of-mass of *n*-pentane. This allowed us to find electronic energies along with relevant structures when the distance between the central molecule in the slab (hereafter denoted *RM*) and the centre of mass (COM) of the slab changed with a step of 0.005 nm. The evaporation starts with the rotation of the methyl group (-CH$_3$) around single bonds of C-C in the backbone of the *n*-pentane. At this stage of the process, the dihedral angle of φ_1 in *RM* changes from 178° in **Re** to 118° in **TS1** and 92° in **Int1**. This means that the structure of *RM* has changed from TT in **Re** in the L phase to GT in **Int1** in the L-G interface. The energy barrier was calculated to be 5 kcal/mol (Figure 4b). The torsion angle φ_1 in **Int2** reached 73° in **Int3**. This single bond rotation, via **TS2**, leads to the formation of the most stable conformer along the reaction pathway (**Int2**). The presence of the **Int2** shows the concept of surface tension in the L-G interface at the site of evaporation. This downhill process (ΔE = -2.8 kcal/mol) proceeds with relatively small barriers ($\Delta E^{\ddagger}$ = 4.4 kcal/mol). For the subsequent step, while φ_1 remains almost constant (70-80°), φ_2 changes from 174° in **Int2** to 94° in **Int3**. This endothermic step (6.3 kcal/mol) occurs with a barrier of 15.7 kcal/mol (**TS3**) in the

interface of L-G showing its rate-limiting step in the evaporation process (Figure 4b). At the last step **Pr** was produced. At this stage *RM* was removed from the slab (its distance was 1.8 nm). It was as stable as **Int4** but much more unstable than **Int3** (Figure 4b) showing a barrier-less step in the evaporation/condensation processes. The energy gap between **Int3** and **Int4** or **Pr** shows that *RM* is near the surface and needs sufficient kinetic energy to be evaporated. Therefore, it can be concluded that evaporation/condensation is not an activated process.

This multi-step process leading to accurate estimation of the evaporation coefficient cannot be limited by only one value even under constant thermodynamic conditions. We aim to extend this work in the future by studying the dynamics of these processes with reliable QC potentials. These QC results are expected to enable us to estimate the evaporation/condensation coefficients more accurately than was done earlier (11-12).

4- Conclusion

Our QC calculations in the gas phase show that *conformerization* energies in *n*-alkanes are mainly responsible for the reduction of the HOMO-LUMO gap since their contribution increases dramatically with increasing chain length of *n*-alkane molecules. We have found that evaporation of *n*-alkanes is a multi-step complex process for which the transformation of a molecule from L to L-G is considered as an activation process and a barrier-less process occurs during the transition from L-G to G. While phase transformations between L and L-G are estimated as activation processes, it is found that there is no energy barrier in the transition between L-G and G.

A double hybrid DFT as a cost-effective potential is suggested for studying the dynamics of evaporation of *n*-alkanes. In this approach all important processes are taken into account (effects of exchange, correlation, dispersion and also spin component contributions of electrons).

Acknowledgements

References

1. V. Formisano, S. Atreya, Detection of methane in the atmosphere of Mars. Science. 306, 1758 (2004).
2. S. S. Sazhin, J.-F. Xie, A kinetic model of droplet heating and evaporation: Effects of inelastic collisions and a non-unity evaporation coefficient. Int. J Heat Mass Transfer. 56, 525–537 (2013).
3. I. Cacelli, G. Prampolini, Parameterization and validation of intramolecular force fields derived from DFT calculations. J. Chem. Theory Comput. 3, 1803-1817 (2007).
4. B. Eckl, J. Vrabec, Set of molecular models based on quantum mechanical *ab initio* calculations and thermodynamic data. J. Phys. Chem. B 112, 12710-12721 (2008).
5. L. L. Thomas, T. J. Christakis, Conformation of alkanes in the gas phase and pure liquids. J. Phys. Chem. B. 110, 21198 (2006).
6. S. W. L. Siu, K. Pluhackova, Optimization of the OPLS-AA force field for long hydrocarbons J. Chem. Theory Comput. 8, 1459-1470 (2012).
7. W. L. Jorgensen, J. D. Madura, Optimized intermolecular potential functions for liquid hydrocarbons. J. Am. Chem. Soc. 106, 813 (1984).
8. W. L. Jorgensen, J. D. Madura, Development and testing of the OPLS all-atom force field on conformational energetics and properties of organic liquids J. Am. Chem. Soc. 118, 11225-11236 (1996)**.**
9. J. I. Siepmann, S. Karaborni, Simulating the critical behaviour of complex fluids. Nature. 365, 330 (1993).
10. D. H. de Jong, G. Singh, Improved parameters for the Martini coarse-grained protein force field. J. Chem. Theor. Comp. 9:687-697 (2013).
11. B. -Y. Cao, J.-F. Xie, Molecular dynamics study on evaporation and condensation of *n*-dodecane at liquid–vapor phase Equilibria. J. Chem. Phys. 134, 164309 (2011).
12. J.-F. Xie, S. S. Sazhin, Molecular dynamics study of the processes in the vicinity of the *n*-dodecane vapour/liquid interface. Phys. Fluid. 23, 112104 (2011).
13. J. M. L. Martin, What can we learn about dispersion from the conformer surface of *n*-pentane? J Phys. Chem. A. 117:3118-32 (2013).
14. A. Salam, M. S. Deleuze, High-level theoretical study of the conformational equilibrium of *n*-pentane. J. Chem. Phys. 116, 1296−1302 (2002).
15. P. Mencarelli, The conformational behaviour of *n*-pentane: A molecular mechanics and molecular dynamics experiment. J. Chem. Educ. 72, 511 (1995).
16. Nils O. B. Luettschwager, The last globally stable extended alkane. Angewandte Chemie-International Edition. 52, 463-466 (2013).
17. B. Smit, S. Karaborni, Computer simulation of vapor-liquid phase equilibria of *n*-alkanes. J. Chem. Phys. 102, 2126-2140 (1995).

18. B. Smit, S. Karaborni, 'Erratum' Computer simulation of vapor-liquid phase equilibria of *n*-alkanes. J. Chem. Phys. 109, 352 (1998).

19. M. G. Martin, J. I. Siepmann, Transferable potentials for phase equilibria. 1. United-atom description of *n*-alkanes. J. Phys. Chem. B. 102, 2569-2577 (1998).

20. A. Katie, J. Ilja Siepmann, Transferable potentials for phase equilibria-coarse-grain description for linear alkanes. J. Phys. Chem. B. 115, 3452–3465 (2011).

21. B. Chen, J. I. Siepmann, Transferable potentials for phase equilibria. 3. Explicit-hydrogen description of *n*-alkanes, J. Phys. Chem. B, 103, 5370-5379 (1999).

22. N. Rai, J. I. Siepmann, Transferable potentials for phase equilibria. 10. Explicit-hydrogen description of substituted benzenes and polycyclic aromatic compounds, J. Phys. Chem. B, 117, 273-288 (2013).

23. C. D. Wick, M. G. Martin, Transferable potentials for phase equilibria. 4. United-atom description of linear and branched alkenes and of alkylbenzenes, J. Phys. Chem. B, 104, 8008-8016 (2000).

24. M. G. Martin, J. I. Siepmann, Novel configurational-bias Monte Carlo method for branched molecules. Transferable potentials for phase equilibria. 2. United-atom description of branched alkanes, J. Phys. Chem. B, 103, 4508-4517 (1999).

25. J. W. Au, G. Cooper, The valence shell photo absorption of the linear alkanes, C_nH_{2n+2} (n= 1-8): absolute oscillator strengths (7-220eV). Chem. Phys. 173, 209-239 (1993).

26. B. A. Lombos, P. Sauvageau, The electronic spectra of *n*-alkanes. J. Mol. Spect. 24, 253-269 (1967).

27. B. A. Lombos, P. Sauvageau, The electronic spectra of normal paraffine hydrocarbons. Chem. Phys. Let. 7, 42-43 (1967).

28. M. J. Frisch, G. W. Trucks, Gaussian 09 Revision A.02 Gaussian, Inc.: Wallingford, CT, 2009.

29. M. S. Gordon, M. W. Schmidt, In: C. E. Dykstra, G. Frenking, K. S. Kim, G. E. Scuseria, editors, Theory and Applications of Computational Chemistry, the First Forty Years Amsterdam: Elsevier. pp. 1167-1189 (2005).

30. R. Dennington, R. GaussView, version 3.07 ed.; Semichem, Inc.: Shawnee Mission, KS, 2003.

31. M. P. Repasky, J. Chandrasekhar, PDDG/PM3 and PDDG/MNDO: Improved semiempirical methods. Journal of Computational Chemistry. 23, 1601-1622 (2002).

32. S. Tsuzuki, K. Honda, Estimated MP2 and CCSD (T) interaction energies of *n*-alkane dimers at the basis set limit: Comparison of the methods of Helgaker et al. and Feller. J. Chem. Phys. 124, 114304 (2006).

33. F. Morini, S. Knippenberg, Quantum chemical study of conformational fingerprints in the photoelectron spectra and (e, 2e) electron momentum distributions of *n*-hexane. J. Phys. Chem A. 114, 4400−4417 (2010).

34. S. Knippenberg, Y. R. Huang, Probing molecular conformations in momentum space: The case of *n*-pentane. J. Chem. Phys. 127, 174306 (2007).

35. M. S. Deleuze, W. N. Pang, Probing molecular conformations with electron momentum spectroscopy: The case of *n*-butane. J. Am. Chem. Soc. 123, 4049-4061 (2001).

36. W. N. Pang, J. F. Gao, Valence electron momentum spectroscopy of n-butane. *J. Chem. Phys. 112*, 8043-8052 *(2000)*.

37. D. Gruzman, A. Karton, J. Phys. Chem. A. Performance of *ab initio* and density functional methods for conformational equilibria of C_nH_{2n+2} alkane isomers ($n = 2–8$). 113, 11974 (2009).

38. J. J. P. Stewart, Optimization of parameters for semiempirical methods VI: more modifications to the NDDO approximations and re-optimization of parameters. J Mol Model. 19:1–32 (2013).

39. F. Gharib, R. Nasiri, Fundamentals of chemical kinetics by S. R. Logan, chap. 4. Prentice Hall (1996).

40. S. Kozuch, J. M. Martin, DSD-PBEP86: in search of the best double-hybrid DFT with spin-component scaled MP2 and dispersion corrections. Phys. Chem. Chem. Phys. 13, 20104-20107 (2011).

41. A. Karton, A. Tarnopolsky, Highly accurate first-principles benchmark datasets for the parameterization and validation of density functional and other approximate methods. Derivation of a robust, generally applicable, double-hybrid functional for thermochemistry and thermochemical kinetics. Journal of Physical Chemistry A 112, 12868–12886 (2008).

42. A. Tarnopolsky, A. Karton, Double-hybrid functionals for thermochemical kinetics. Journal of Physical Chemistry A Letters 112, 3–8 (2008)

43. A. Karton, J. M. L. Martin, Basis set convergence of explicitly correlated double-hybrid density functional theory calculations. Journal of Chemical Physics 135, 144119, pp 1–7 (2011).